CHEMMEDCHEM

DOI: 10.1002/cmdc.200600158

Insight into the Inhibition of Human Choline Kinase: Homology Modeling and Molecular Dynamics Simulations

Lara Milanese, Antonio Espinosa, Joaquín M. Campos, Miguel A. Gallo, and Antonio Entrena*[a]

A homology model of human choline kinase (CK-α) based on the X-ray crystallographic structure of C. elegans choline kinase (CKA-2) is presented. Molecular dynamics simulations performed on CK-α confirm the quality of the model, and also support the putative ATP and choline binding sites. A good correlation between the MD results and reported CKA-2 mutagenesis assays has been found for the main residues involved in catalytic activity. Preliminary docking studies performed on the CK-α model indicate that inhibitors can bind to the binding sites of both substrates (ATP and choline). A possible reason for inhibition of choline kinase by Ca^{2+} ion is also proposed.

Introduction

Phosphatidylcholine is the most abundant phospholipid in eukaryotic organisms. It has a structural role as an essential component of cellular membranes and serum lipoproteins, and also a functional one, as a precursor of lipid second messengers.[1] In mammalian cells, phosphatidylcholine can be synthesized de novo by two pathways, the CDP-choline pathway (Kennedy pathway)[2] and the phosphatidylethanolamine methylation pathway.[3]

Choline kinase (CK, ATP:choline phosphotransferase, EC 2.7.1.32) catalyzes the ATP-dependent phosphorylation of choline, the first step in the CDP-choline pathway, and has been reported to regulate this pathway under certain conditions.[4] Genes or cDNAs of choline kinases from different species have been isolated, and the alignment of the deduced protein sequences have revealed several highly conserved regions.[5] In mammalian cells, CK exists in at least three functional isoforms, encoded by two different genes (ck-α and ck-β). All the isoforms are active only in an oligomeric form (di- or tetrameric), and require ATP and Mg^{2+} for their catalytic activity.[6]

Phosphorylcholine (P-Cho), the product of the CK-catalyzed phosphorylation reaction, has been identified as a second messenger required for DNA synthesis induced by growth factors. Increased levels of P-Cho and CK can be observed during the early stages of mitogenic stimulation,[7] and in several mammalian tumors, when compared with their corresponding normal tissues.[8] It has recently been demonstrated that CK inhibitors lead tumor cells to apoptosis, whereas normal cells remain unaffected.[9] This evidence suggests that the inhibition of CK could represent a valid antiproliferative strategy and lead the research towards the development of CK inhibitors.

In this context, in a research project aimed to develop new antiproliferative agents, we have previously synthesized and characterized several symmetrical bis- and tris-cationic compounds of general formulae **1**–**14** shown in Figure 1,[10–15] based on structural modifications of hemicholinium-3 (HC-3), a well known CK inhibitor.

The recently reported crystal structure of a CK isoform (CKA-2) from *C. elegans*,[5] and the correlated site-directed mutagenesis studies,[16] have provided new opportunities to rationalize the knowledge regarding the inhibition of this enzyme. The CKA-2 catalytic domain shows a high degree of similarity to that of other kinases, such as the bacterial aminoglycoside 3′-phosphotransferase [APH(3′)-IIIa][17] and the cAMP-dependent protein kinase A (PKA),[18] with at least two highly conserved motifs: the Brenner phosphotransferase motif, shared by many protein kinases and aminoglycoside phosphotransferase,[19] and the choline kinase motif, characteristic of the choline/ethanolamine kinase family.[20]

The electron-density map of CKA-2 showed a strong solvent peak attributed to a Ca^{2+}, as the protein was crystallized in the presence of 200 mM $CaCl_2$. It has been reported that Ca^{2+} inhibits CK activity,[16] although in the crystal structure of CKA-2 this ion lies at about 10 Å from the putative Mg^{2+}-ATP binding site, too far away for direct competition with Mg^{2+}.[5]

Here we report the construction of a 3D homology model of the human choline kinase CK-α, starting from the crystal structure of CKA-2, as the first stage in the study of the inhibition mechanism of CK-α by our reported molecules. From this model, we constructed several complexes containing ATP and/

[a] *L. Milanese, Dr. A. Espinosa, Dr. J. M. Campos, Dr. M. A. Gallo, Dr. A. Entrena*
Departamento de Química Farmacéutica y Orgánica
Facultad de Farmacia, Campus de Cartuja s/n
Universidad de Granada, 18071 Granada (Spain)
Fax: (+34) 958-243845
E-mail: aentrena@ugr.es

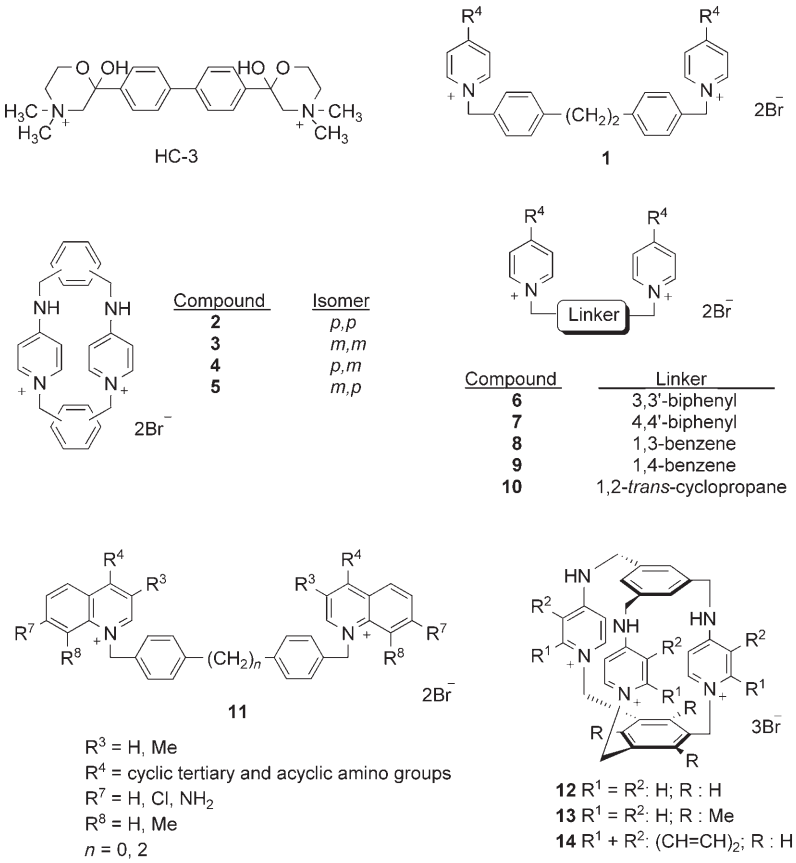

Figure 1. Structures of several human choline kinase (CK-α) inhibitors. Compounds **1**: see ref. [10]; compounds **2**–**5**: see refs. [11] and [14]; compound **2**: see also ref. [15a]; compounds **6**–**10**: see refs. [12] and [14]; compounds **11**: see refs. [13] and [14]; compounds **12**–**14**: see refs. [14] and [15].

or choline and a series of molecular dynamics (MD) simulations were performed, to validate the proposed substrate-binding sites. This information should be useful in the design of new choline kinase inhibitors that could be used as anticancer drugs. On the other hand, our MD studies also furnish a reasonable explanation for the mechanism of Ca^{2+}-mediated inhibition of CK.

Results

Homology model

Figure 2 shows the alignment and the residues used as the template in the construction of the model. It can be seen that CKA-2 and CK-α enzymes are very similar within the secondary structural organization, and that there exists a large number of conserved residues (37% of residues are conserved between CKA-2 and CK-α), particularly those of the two distinctive regions called the Brenner and choline kinase motifs.

The Brenner phosphotransferase motif, $hXHXDhX_3N$ (Figure 2) (where h is a large hydrophobic residue) has been identified in many phosphotransferase enzymes.[19,20] In the known choline/ethanolamine kinases (CK/EK), the residues from this motif have a structural role constituting part of the ATP binding site, and also participate in the orientation of the second substrate (choline in CKA-2 and CK-α). In CKA-2 the Brenner motif can be found on the connecting loop between strands 9 and 10. In this motif CKA2 and CK-α share 92% of conserved residues.

The choline kinase motif, $(LIV)X_2ID(FWY)E(YF)X_3NX_3(FWY)DX_6E$ (Figure 2), is characteristic of the choline/ethanolamine kinase family[18] and in CKA-2 is located on strands 11 and 12 and helix G. It's conserved hydrophilic and aromatic residues are thought to be involved both in catalyzing the reaction and in the orientation of the substrates. CKA2 and CK-α also show a high degree of conserved residues (72%) in this motif.

Almost all the residues that have a significant structural and/or functional role for CKA-2 activity are conserved in CK-α, and it can also be seen that there are four regions that do not match the template molecule.

The first region (region a, Figure 3) is a proline-rich region (PQPPPPQP) situated immediately after the helix A′ (Figure 2). This region could possibly play some role in the recognition of the protein surface, but as our purpose is only to validate the enzyme putative binding sites, we decided to model this octamer as an external loop that points outside the protein and does not alter the overall structure.

The second region, situated between sheet 3 and helix B (Figure 2), contains 22 amino acids and is the longest one. This region has been modeled by searching fragments that match its sequence in the crystal structures found in the Brookhaven Protein Data Bank. In the final model, this region contains a new helix denoted as B′, whose secondary structure was predicted by the Jpred server, and a loop between this new helix B′ and the helix B is denoted as b in Figure 3. This region is also situated outside the protein and does not significantly alter the overall structure.

The third region corresponds to a 30 residue CKA-2 fragment that is situated between β-strands 10 and 11 (Figure 2). The 3D structure of this region is not resolved in the CKA2 crystal structure, indicating high mobility of these residues. Nevertheless, the location of both strands 10 and 11 in the CKA2 crystal structure indicate that these 30 residues are probably oriented outside the enzyme. The corresponding sequence in CK-α is shorter (8 residues) and was modeled as a loop joining the two strands and also oriented outside the enzyme (Figure 3, region c).

Finally, the fourth region is situated between CKA-2 helix H and I, and is a short region of four amino acids (ENLS) that has been modeled as a loop denoted with letter d in Figure 3, and also pointing outside the protein. This loop introduces only a small difference between the 3D structures of both enzymes: in CKA-2 helix I and J are aligned forming a continuous helix, while in the CK-α model the axes of these helixes form an angle close to 170 degrees. Nevertheless, this small modification does not affect the main part of the protein: the Brenner and the CK motifs.

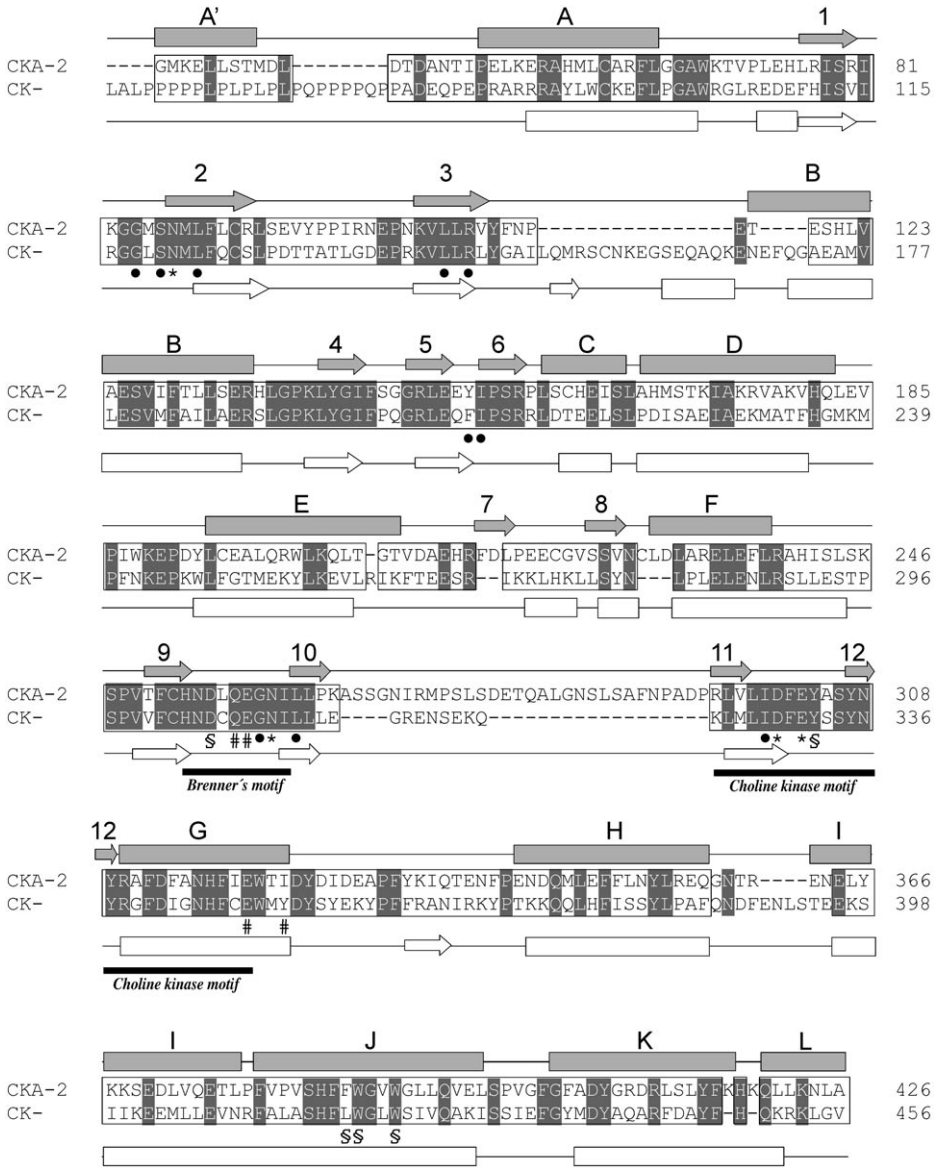

Figure 2. Primary structural alignment of *C. elegans* choline kinase CKA-2 and human CK-α (CLUSTAL W, alignment score 880). Residues whose coordinates have been used as a template for the three-dimensional homology model construction are included in black borders. Residues highlighted in gray are conserved between the two sequences. Experimental secondary structure of CKA-2 is represented by gray boxes (α-helices, labeled by letters) and arrows (β-strands, labeled by numbers). Predicted secondary structure for CK-α was represented by white boxes (α-helices) and arrows (β-strands). Residues involved in the binding with the substrates are indicated as follows: [*] for residues binding Mg^{2+} ions; [●] for residues binding ATP; [§] for residues constituting the proposed choline binding site; and [#] for residues binding Ca^{2+} ion. The string between β-strands 10 and 11, not resolved in the crystal structure of CKA-2, is indicated by typing the residues in italics.

The quality of the 3D structure has been tested using the Verify 3D server.[21] Figure 4 shows the average score value for each residue and only some residues belonging to the four external loops a, b, c, and d give values smaller than 0.2, indicating that the model is correct.

Molecular dynamics simulations

Two molecular dynamics simulations have been tackled to validate the CK-α model and the putative ATP and choline binding sites, to understand the interactions between the CK-α residues and both substrates, and to interpret the role of Ca^{2+} ion in the inhibition of the CK catalytic activity. Table 1 shows the composition of each complex prepared for simulations A and B. Simulation A was tackled to test the hypothesis regarding the ATP and choline binding sites and its suitability as a model regarding the catalytic mechanism. Simulation B has been performed with the purpose of studying the role of Ca^{2+} on the inhibition of the catalytic activity.

It has been observed that both systems remain stable during the 2 ns simulation time. Table 1 also shows the root mean square deviation (rmsd) calculated over the backbone atoms between the average molecular dynamics structure of each simulation and the CK-α homology model. System A, where both substrates and Mg^{2+} ions are present, shows the smallest value (2.44 ± 0.29 Å), while system B shows the highest rmsd values (2.78 ± 0.33 Å). In general the rmsd values are relatively high, but this fact is mainly due to the movement of the external loops, introduced in the construction of the CK-α model (vide supra), that show a higher mobility in relation to the conserved region. It must be noted that the presence of Ca^{2+} ion produces a higher deviation in the backbone of the protein in relation to the corresponding simulation without the ion.

The values of the radius of gyration indicate a good stability, a slight expansion of the protein can even be observed when compared with the CK-α model. In fact, the radius of gyration for our CK-α model is 21.48 Å, similar to the value of 21.09 Å calculated for the CKA-2 crystal structure. For simulations A and B, higher values of the radius of gyration can be observed because of the expected expansion necessary to accommodate both substrates. An inspection of the variation of the radius of gyration during the trajectory indicates that the difference is due to the Ca^{2+} ion. Figure 4 shows the variation of the radius for simulations A and B against time, and it can be seen that in

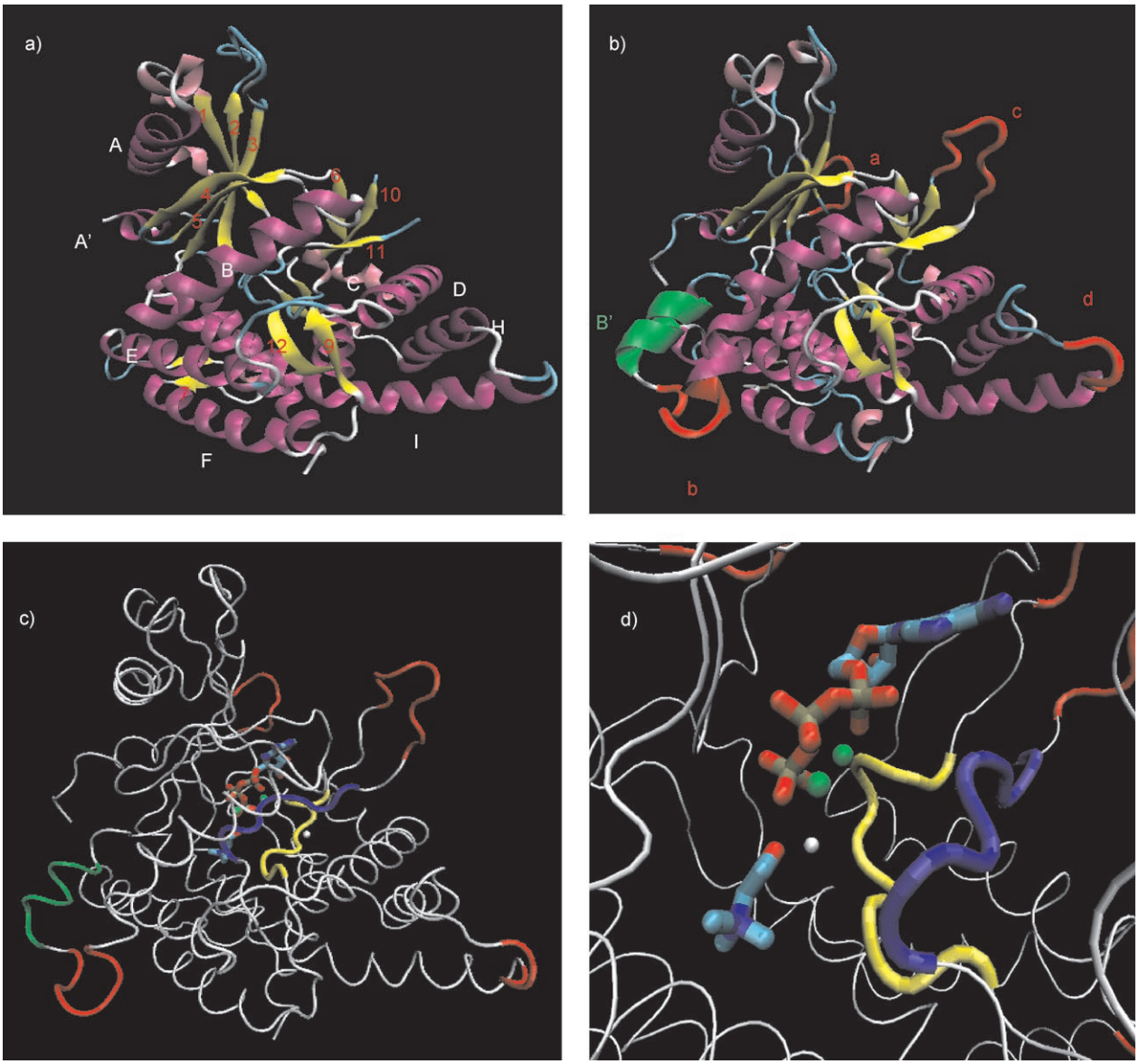

Figure 3. a) 3D structure of the CKA-2. b) 3D model of the human CK-α showing the secondary structure (purple: helices, yellow: sheets, white: loops). The additional fragments inserted in the CK-α model are shown, the helix B′ in green and the external loops (a, b, c, and d) in red. c) Situation of the ATP and choline inside the CK-α model in relation to the Brenner's (yellow) and choline kinase (blue) motifs. d) A more detailed view showing the situation of Mg^{2+} (green sphere) and Ca^{2+} (white sphere) ions.

the presence of Ca^{2+} the radius grows more slowly, indicating that the enzyme becomes more rigid.

Putative ATP binding site

The proposed ATP binding pocket[5] is formed by the helix B, the loop between strands 1 and 2, the β sheet made up of strands 6, 10, and 11, and the loop between strands 11 and 12 (Figure 2). In addition, this pocket is defined by highly conserved residues and the mutation of some of them often leads to a decreased catalytic efficiency and/or affinity for ATP.[16] The same pocket also includes the two Mg^{2+} ions required for catalytic activity.

Two slightly different modes for the Mg^{2+} binding evolve during the simulations, depending on the presence or absence of the Ca^{2+} ion.

In system B, where calcium was inserted into the protein, both Mg^{2+} ions are coordinated with six oxygen atoms (Figure 5). One of them (Mg-1) coordinates two O atoms belonging to the second (O2B) and third (O3G) ATP phosphate moieties, the two O atoms (OE1 and OE2) of the Glu 331 carboxylate moiety, one O atom (OD1) of the Asp 329 carboxylate group, and the O atom (OD1) of Asn 121 (strand 2). The second magnesium (Mg-2) coordinates with two O atoms from the first (O2A) and third (O1G) ATP phosphate moieties, the second O atom (OD2) of Asp 329 carboxylate moiety, the O atom (OD1) of Asn 310, and the O atom of two water (WAT)

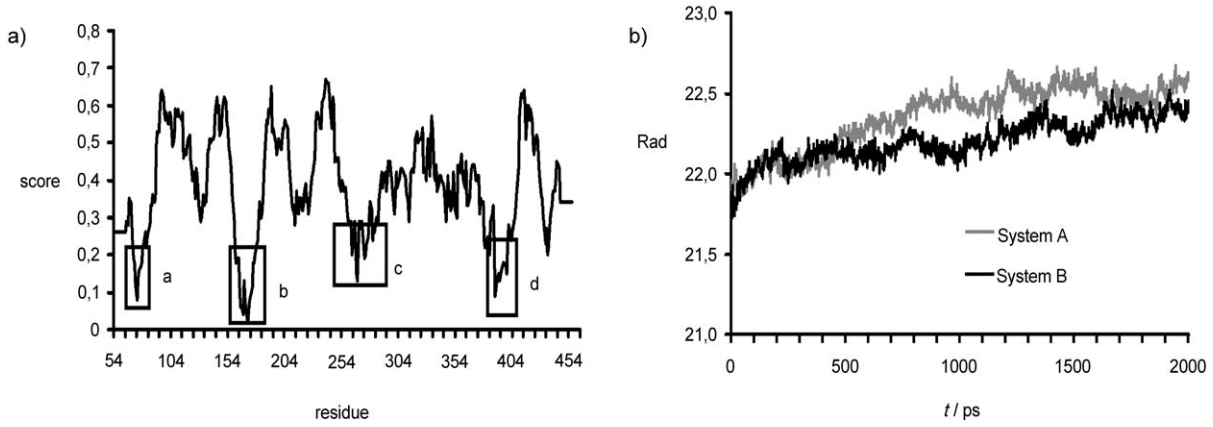

Figure 4. a) Graph representing the Verify 3D score for the CK-α model. Only four zones of the protein with low score have been found and correspond to the four external loops a, b, c and d. b) Variation of the radius of gyration (Rad, Å) versus time for simulations A (gray) and B (black). A steady expansion of the enzyme necessary to accommodate the substrates can be observed in both systems, being smaller in system B because of the presence of a Ca^{2+} ion.

Table 1. Summary of the molecular dynamics simulations.

Simulation	System	No. Atoms	Radius of Gyration [Å]	rmsd [Å]
A	CK-α, ATP, 2 Mg^{2+}, Choline, 2 Na^{+}, water	30824	22.21 ± 0.20	2.44 ± 0.29
B	CK-α, ATP, 2 Mg^{2+}, Choline, Ca^{2+}, water	30823	22.14 ± 0.13	2.78 ± 0.33

molecules. Glu 331 and Asp 329 are situated in the choline kinase motif, whereas Asn 310 belongs to the Brenner motif.

In system A (no calcium present) a slightly different situation has been found as an additional amino acid plays a role that could be crucial for the catalytic activity (Figure 5). The absence of the Ca^{2+} ion allows Gln 307, a conserved residue located in the Brenner motif, to shift toward Mg-2 and establish a coordinated bond between its O atom (OE1) and this magnesium ion. In simulation B, this residue remains firmly bound to the calcium ion and does not participate in the coordination with magnesium. The Gln 307 movement produces a displacement of Asn 310, Asp 329, Glu 331, and Asn 121. Asn 310 (OD1) continues to coordinate Mg-2, but the interaction between Mg-2 and Asp 329 is lost and Asp 329 (OD1) remains bonded only to Mg-1. On the other hand, Mg-1 coordinates with only one O atom (OE1) of Glu 331 whereas Asn 310 does not participate in the coordination with Mg-1. Finally, Mg-1 binds three oxygen atoms belonging to each one of the ATP phosphate groups (O1A, O2B, and O3G, respectively).

All these interactions remain stable during the entire 2 ns trajectory, with average values that are compatible with the coordinated bonds described (Table 2). Only the distance between one of the water molecules and Mg-2 shows abnormally

Table 2. Average time distances [Å] for the main interactions between ATP, choline, Mg and Ca in MD simulations A and B.

Ligand	Residue	System A	System B	Ligand	Residue	System A	System B
Mg-1	Asn 121 (OD1)	–	2.11 ± 0.10	ATP(O4)	Gly 118 (H)	–	2.03 ± 0.22
	Asp 329 (OD1)	1.91 ± 0.05	1.92 ± 0.05	(N1)	Ile 208 (H)	1.97 ± 0.12	2.03 ± 0.14
	Glu 331 (OE1)	1.86 ± 0.04	1.89 ± 0.05	(3OH)	Gly 309 (O)	2.75 ± 1.22[b]	2.33 ± 1.09
	Glu 331 (OE2)	–	1.98 ± 0.07	(O2G)	Ser 120 (HG)	1.75 ± 0.32	1.71 ± 0.11
	ATP (O1A)	1.95 ± 0.06	–	(O3B)	Ser 120 (H)	2.54 ± 0.32[b]	1.91 ± 0.12
	ATP (O2B)	1.86 ± 0.04	1.83 ± 0.04	(O1B)	Asn 121 (H)	2.02 ± 0.21	1.97 ± 0.13
	ATP (O3G)	1.83 ± 0.03	1.85 ± 0.04	(O1B)	Asn 121(HD2)	5.03 ± 1.46[c]	-
				(O1B)	Arg 145(HH1)	–	2.31 ± 0.20
				(O1 A)	Arg 145(HH2)	2.14 ± 0.29	1.82 ± 0.11
				(O3G)	Tyr 332 (HH)	–	1.90 ± 0.17
Mg-2	Asp 310 (OD1)	2.01 ± 0.07	2.06 ± 0.09	Ca	Gln 307 (OE1)	–	2.38 ± 0.08
	Asp 329 (OD2)	–	1.89 ± 0.05		Glu 308 (OE1)	–	2.30 ± 0.07
	Gln 307 (OE1)	1.97 ± 0.06	–		Glu 308 (OE2)	–	2.26 ± 0.06
	ATP (O1B)	1.82 ± 0.04	1.82 ± 0.04		Glu 348 (O)	–	2.35 ± 0.08
	ATP (O3B)	1.85 ± 0.04	1.85 ± 0.04		Glu 348 (OE1)	–	2.21 ± 0.05
	WAT	2.03 ± 0.06	2.03 ± 0.07		Tyr 351 (O)	–	2.35 ± 0.07
	WAT	9.11 ± 12.81[a]	7.84 ± 10.89[a]				

[a] The water molecule approaches the Mg-2 ion during the simulation. [b] This interaction is stable only during some periods of the dynamic simulation. [c] This interaction appears only during the last 0.5 ns of the trajectory, and for this period the value of the distance is of 2.01 ± 0.31.

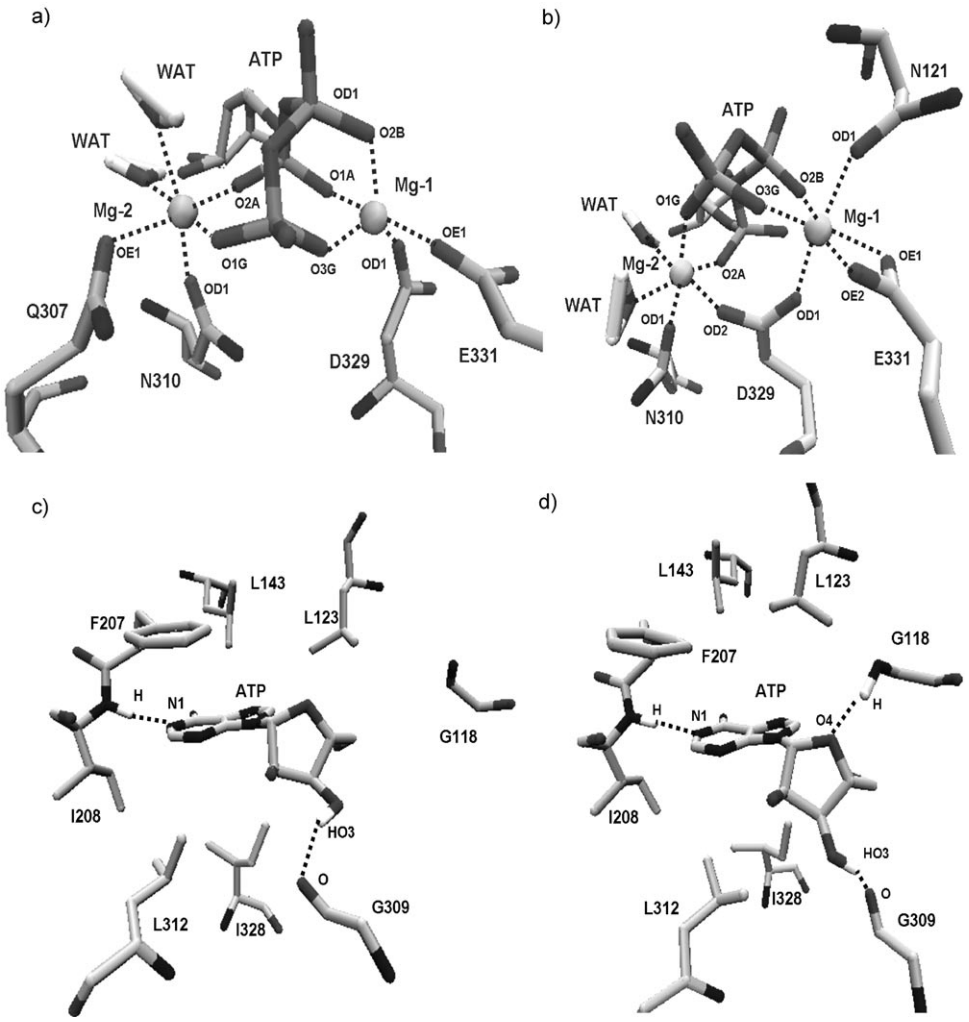

Figure 5. a) Coordination of both Mg^{2+} ions in simulations A. b) Coordination of Mg^{2+} ions in simulation B. The role of Gln 307 can be clearly observed in simulation A. c) Detailed view of all residues that interact with ATP adenine and ribose moieties in system A. d) The same representation for system B.

high values for the distance and the standard deviation, indicating the approach of that water molecule to the ion during the dynamics simulation.

On the other hand, ATP also interacts directly with some residues of the protein. Figure 5 also shows the part of the ATP binding site corresponding to the adenine and ribose moieties. It can be seen that the adenine moiety is accommodated in a hydrophobic pocket formed by Leu 123 (strand 2), Leu 143 (strand 3), Phe 207 and Ile 208 (strand 6), Leu 312 (Brenner's motif), and Ile 328 (choline kinase motif). All these residues are conserved in CKA2, human, and mouse choline/ethanolamine kinases (CK/EK), with the exception of Phe 207 that is substituted by a tyrosine in the last three enzymes. Stabilization of the adenine is due to the van der Waals interactions with these hydrophobic residues, a π,π staking with the Phe 207 side chain, and the formation of a hydrogen bond between the Ile208 NH backbone and adenine N-1 atom. The adenine binding mode inside the enzyme does not depend on the presence or absence of Ca^{2+} ion as it has been found to be similar in both molecular dynamics simulations A and B. The average distance for the Ile 208-N1 hydrogen bond varies from 1.97 Å in system A to 2.03 Å in system D (Table 2).

Interactions between the ribose moiety and the enzyme are slightly different for simulations A and B, depending on the presence of Ca^{2+} ion (Figure 5). In simulation B, two hydrogen bonds are formed, the first one between the ribofuranoside O atom (O4) and the NH backbone of Gly 118 (H), situated on the loop between strands 1 and 2, and the second one between the ribose 3OH group (HO3) and the CO backbone of Gly 309 (O), belonging to the Brenner motif. These two amino acids are also conserved in CKA-2 and in human and mouse EK/CKs. Nevertheless, in the absence of the Ca^{2+} ion only the second hydrogen bond is found in simulation A (average distance 2.75 ± 1.22 Å, Table 2). As mentioned above, in simulation A, Gln 307 moves toward the second Mg^{2+} ion, and this movement can alter the conformation of Gly 118 in such a way that the hydrogen bond with the O4 group cannot take place, and this is probably the reason for the difference in the behavior of both systems A and B.

Finally, the phosphate groups also interact with the enzyme through several residues and these interactions have proved to be more variable (Figure 6). In the more rigid system B, four residues participate by means of hydrogen bonds in the stabilization of the three ATP phosphate groups. First, Arg 145 (strand 3), forms two hydrogen bonds (HH1 and HH2 atoms) with one oxygen atom belonging to each of the first (O1A) and second (O1B) phosphate units. The second residue is Asn 121 (strand 2) that also forms one hydrogen bond between its NH backbone (H) and the same O atom (O1B) of the second phosphate group that is bound to Arg 145. Third, Ser 120 (strand 2) forms two hydrogen bonds, one of them between the OH group (HG) and one O atom (O2G) of the third phosphate, and the other between the NH of the backbone (H) and the O atom that join the second and the third phosphate groups (O3B). Finally, the fourth residue is Tyr 332, situated on the CK motif and one of the amino acid that defines the choline binding pocket (vide infra), and gives rise to a hydrogen bond between its OH group (HH) and one O atom (O3G) of the last phosphate moiety. All these five hydrogen bonds

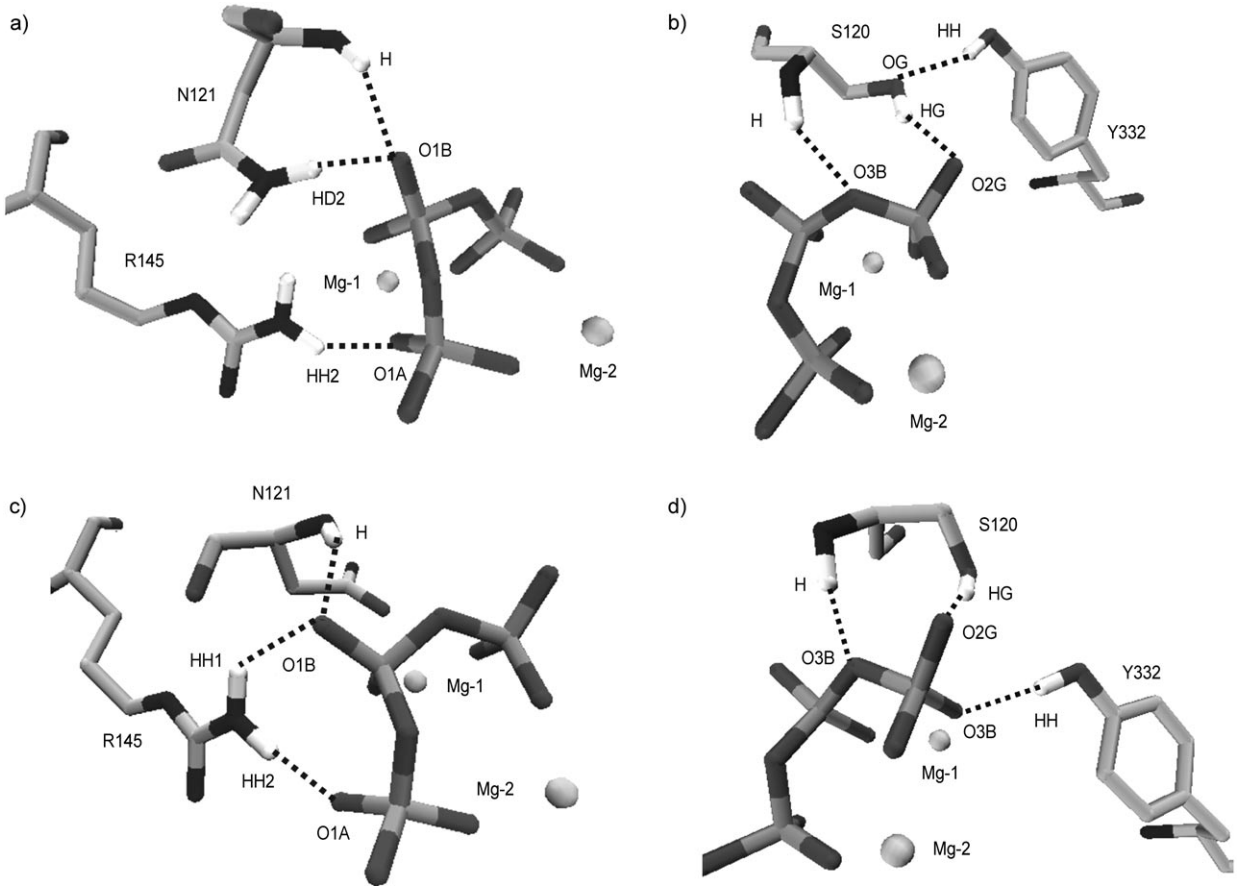

Figure 6. a) and b) Two detailed views of the residues involved in the interaction with the phosphate moieties in system A. c) and d) The equivalent interactions for simulation B.

remain stable during the 2 ns of the trajectory, with average distances concordant with the presence of such hydrogen bonds (Table 2).

In system A the situation is slightly different. Arg 145 forms only one hydrogen bond (HH2) with the first phosphate group (O1A) and Ser 120 still participates in the same two hydrogen bonds. Tyr 332 no longer participates in the hydrogen bond with the ATP terminal phosphate moiety and forms a hydrogen bond with the OH group of Ser 120 (2.38 ± 0.51 Å). Finally, Asn 121 continues to form the hydrogen bond between the NH backbone (H) and the second phosphate (O1B). Nevertheless, Asn 121 does not participate in the coordination with Mg-1 in this simulation, and a rotation of the side chain is observed in such a way that this residue also forms an additional hydrogen bond with the O atom (O1B) of the second phosphate by means of one of its NH2 hydrogen atoms (HD2). This second hydrogen bond is formed during the last 0.4 ns of the trajectory, and this situation must again be attributed to the reorganization in the Mg^{2+} coordination due to the movement of Gln 307.

Putative choline binding site

The putative choline binding site is located at the domain interface of the molecule delimitated by the loop between helices G and H, the reverse turn between helices I and J, and the loop between strands 1 and 2, and is connected to the proposed ATP binding site. This pocket is defined by residues Tyr 332, already mentioned in the interaction with the terminal ATP phosphate moiety, Leu 418, Trp 419, and Trp 422, residues situated on helix J. Both Trp amino acids are highly conserved in CKA2, CK-α, human, and mouse EK/CK, whereas Leu 418 is substituted by a Phe in these three enzymes. These residues define a pocket where the choline positive charge can easily be stabilized by means of π-cation interactions. In both simulations A and B, stabilization of choline in the binding site and the proper orientation of the terminal ATP phosphate unit have been clearly observed (Figure 7).

Figure 7 also shows the position of Asp 305, a residue belonging to the Brenner motif and highly conserved in CKA-2, CK-α, protein kinases, EK/CKs, and APH(3′)-IIIa. This Asp is a critical residue in the catalytic process of such enzymes although its role is not clearly demonstrated. It has been proposed that it can act as a base taking the proton from the incoming substrate hydroxy group[22] or that it is involved in the appropriate orientation of the substrate.[23]

In our simulations, Asp 305 is near enough to the choline molecule and can act by means of the two proposed mechanisms. In simulation A, the situation of Asp 305 seems to be more appropriate for the catalysis as it points directly to the

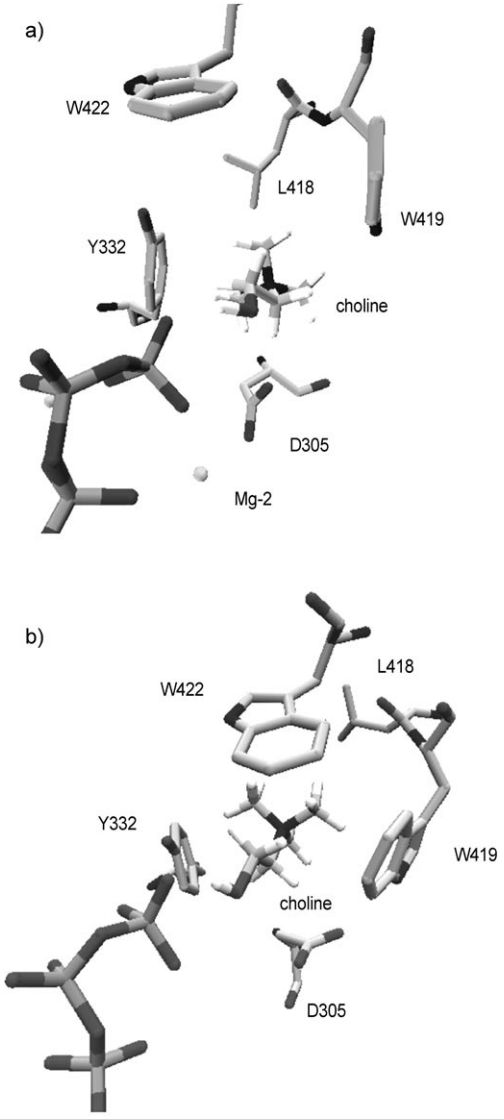

Figure 7. a) and b) Detailed views of the choline binding site in simulations A and B, respectively.

choline OH group. In fact, only a small rotation of the hydroxy group is needed to allow the transference of the proton to Asp 305. Nevertheless, in simulation B the Asp 305 is pointing in a slightly different direction that seems to be less appropriate for the deprotonation of choline.

Ca^{2+} binding

In the crystal structure of CKA-2, the Ca^{2+} ion is pentacoordinated, making bonds with the carboxylate moieties of E258 (two bonds) and E320 (one bond), and with the backbone carbonyl groups of E320 (one bond) and I323 (one bond).[24] Because Ca^{2+} ions normally form octahedral coordination, it has been argued that the sixth ligand should be a water molecule that was not observed in the X-ray experiment. Nevertheless, this possibility does not seem to be probable, as in the crystal structure of CKA-2 several other water molecules (341 in total) surrounding the protein are observed, none of them coordinated with Ca^{2+} ion.

The two first CKA-2 amino acids (E258 and E320) are conserved in CK-α and correspond to Glu 308 (Brenner's motif) and Glu 348 (helix G). On the other hand, I323 is mutated into Tyr 357, also situated on helix G, but this mutation is not very important as the coordination with calcium takes place through the backbone carbonyl oxygen atom.

In simulation B, the Ca^{2+} ion was initially situated inside the CK-α model on an equivalent position to CKA-2 crystal structure, making bonds with Glu 308 (two bonds with OE1 and OE2 atoms), Glu 348 (one with the O backbone atom and another with one carboxylate OE1 atom), and Tyr 357 (one bond with the O backbone atom).

The most interesting finding in this simulation is that during the equilibration period a movement of Gln 307 (also in Brenner's motif) can be observed so that the backbone O atom of this residue makes a new bond with the Ca^{2+} ion, thus completing the octahedral coordination of the ion.

Figure 8 shows the average structure for simulation B where the hexacoordination of the Ca^{2+} ion can be observed. This situation remains stable during the 2 ns of both simulations with the Ca^{2+}-O average distance of about 2.30 Å (Table 2).

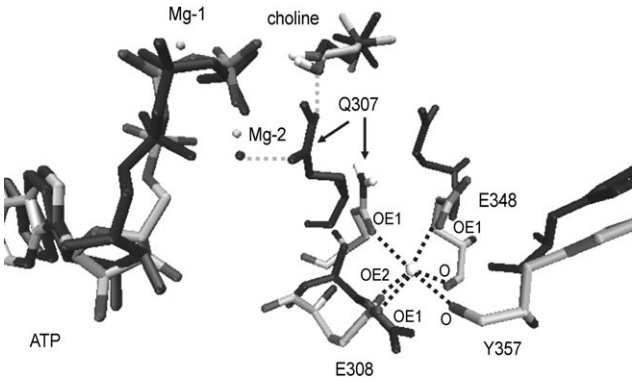

Figure 8. Superposition of the average structures of simulations A (black) and B (gray). In simulation B, the Ca^{2+} ion coordination is fulfilled by Tyr 357 (O), Glu 348 (O and OE1), Glu 308 (OE1 and OE2) and Gln 307 (OE1). In simulation A, the three first residues move freely, but Gln 307 (indicated by arrows) rotates, coordinates one of the Mg^{2+} ion and stabilizes the choline molecule.

Nevertheless, in simulation A (no Ca^{2+} ion) all the residues that interact with the ion show a higher mobility, and the Gln 307 rotates in the opposite direction and coordinates with one of the Mg^{2+} ions that binds the ATP molecule. This movement alters the coordination in both Mg^{2+} ions and the ATP binding (vide supra), and also modifies the ATP and choline binding, as the Gln 307 NH_2 group forms an additional hydrogen bond with the choline O atom. Figure 8 shows the average structure for simulation A in which the orientation of Gln 307 coordinates to the Mg^{2+} and the interaction with choline is clearly visible.

Table 3. Summary of the residue mutations performed on CKA-2 and their influence on the activity.[a] The equivalence between the CKA-2 and CK-α residues is indicated.

Region	CKA-2	CK-α	Mutation	Effect
NH2-terminal	S86	Ser 120	S86A	Pronounced reduction of the catalytic efficiency (k_{cat}/K_m)
			S86T	Moderate reduction of the catalytic efficiency (k_{cat}/K_m)
	N87	Asn 121	N87A	Small reduction of the catalytic efficiency.
	R111	Arg 145	R111A	4-fold increase in Km for ATP.
	E125	Glu 179	E125A	Modest reduction of K_{cat} and Km for ATP
			E125Q	Modest reduction of K_{cat} and Km for ATP
			E125D	No influence
	R149	Arg 203	R149A	No influence
Brenner's motif	H253	His 303	H253A	Similar initial activity, but time instability.
	N254	Asn 304	N254A	Similar initial activity, but time instability.
	D255	Asp 305	D255A	Complete loss of activity
			D255N	Small residual activity
			D255E	Small residual activity
	N260	Asn 310	N260A	Small residual activity
CK motif	D301	Asp 329	D301A	Complete loss of activity
			D301N	Complete loss of activity
			D301E	Complete loss of activity
	E303	Glu 331	E303A	Strong reduction of the catalytic efficiency
			E303D	Small reduction of k_{cat}
			E303N	Small reduction of k_{cat}
	N308	Asn 336	N308 A	Small reduction of k_{cat}
			N308D	Modest reduction of k_{cat}
			N308Q	Modest reduction of k_{cat}
	E320	Glu 348	E320A	Reduction of ATP affinity and time instability
COOH-terminal	W387	Trp 419	W387A	Strong reduction of k_{cat} (30-fold)

[a] All biological data are taken from reference [16].

Discussion

In this paper we present a 3D homology model of human CK-α based on the crystal structure of CKA-2. Both enzymes show a high degree of homology and, in particular, the main residues of the Brenner and the CK motifs are conserved in both enzymes. Only four external loops and an additional fragment with an α-helix structure (also externally situated), have been added to the homology model to complete the CK-α 3D structure. The high score of the model measured in the Verify 3D server supports the quality of the structure. Also, the model has been demonstrated to be stable in a 2 ns molecular dynamics simulation.

Like CKA-2, CK-α shows a high degree of similarity with other kinases, and putative binding sites for ATP and choline have been proposed according to those previously proposed for CKA-2. Our molecular dynamics simulations support the availability of these binding sites.

A recent study describes the mutation of several residues in CKA-2 and identifies the role of these amino acids in the catalytic process.[16] Table 3 summarizes the mutated residues, the effect on catalysis, expressed as the reduction of the catalytic efficiency (k_{cat}/K_m) or as the reduction in the ATP or choline affinity (increment of the K_m value), and the equivalent CK-α residue.

In the NH_2-terminal region of the enzyme, the mutation of CKA-2 S86 by an alanine (S86A) produces a strong diminution of the catalytic efficiency for both substrates, whereas the mutation by a threonine (S86T) is less detrimental, indicating that a hydroxy group is necessary for the activity in this position. This residue is conserved in CK-α (Ser 120) and in our model, directly stabilizes the ATP molecule by means of two hydrogen bonds (Figure 6). Substitution of this residue by an Ala should prevent the formation of the hydrogen bond by the Ser 120 hydroxy group, diminish k_{cat}, increase ATP K_m, and give rise to poor catalytic activity. This mutation also diminishes the affinity for choline, and this can be an indirect effect due to the lack of stabilization of the terminal ATP phosphate moiety. On the other hand, a mutual stabilization between the choline and the last ATP phosphate unit can be expected, and consequently a higher mobility of the phosphate because of the Ser mutation should also diminish the K_m for choline. Finally, mutation by a threonine still allows the formation of both hydrogen bonds and consequently, higher catalytic activity.

The mutation of CKA-2 N87 by an Ala (N87A) is less critical for the activity than the mutation of S86, as it produces only a small reduction of the catalytic efficiency. This residue is also conserved in CK-α and corresponds to Asn 121. In our model we have found that the interaction with ATP forms a hydrogen bond through the NH backbone (Figure 6), and consequently the nature of the side chain is not so important.

Mutation of CKA-2 R111 by alanine (R111A) gives rise to a fourfold increase in K_m for ATP, indicating a significant lost of affinity for this substrate. In our model, the corresponding residue is Arg 145, which directly interacts with ATP forming hydrogen bonds between its side chain and the ATP phosphate units (Figure 6). Consequently, mutation of this residue prevents the ATP stabilization and diminishes the affinity for this substrate.

Two other conserved residues of the N-terminal domain that have been mutated in CKA-2 are E125 and R149. E125A or E125Q mutations result in moderate effects on both k_{cat} and K_m for ATP, while the E125D mutation was not detrimental to activity. In our model, this residue is also conserved (Glu 179), but it is situated far from all the substrates and ions, as in CKA2, and consequently its role in the catalysis could not be easily explained. R149A mutation does not significantly affect the catalytic efficiency of the enzyme and hence, this residue is not important for activity. This residue is also conserved in CK-α (Arg 203), but does not interact with any substrates or ion.

On the Brenner motif of CKA-2, H253, and N254 have been mutated into alanine, and in both cases (H253A and N254A) the initial catalytic activity of the mutant enzymes is similar to that of the native one. Nevertheless, these mutants only exhibit stability in the enzyme assay for a few seconds, indicating a structural role for both of them. In fact, H253 is involved in a hydrogen bond network with other residues, including H181 situated on helix D, H253, N254, and D255 belonging to Brenner's motif, and I300, D301, N308, and D313 on the CK motif. All these residues are conserved in CK-α, and correspond to His 235, His 303, Asn 304, Asp 305, Ile 328, Asp 329, Asn 336, and Asp 341, respectively. Figure 9 shows the hydrogen-bond network in the CK-α model. His 235 forms a hydrogen bond with one O atom of Asp 341, which in turn hydrogen bonds the NH backbone of His 303 and Asn 304. His 303 forms two hydrogen bonds with the NH backbone of Asp 305 and the CO backbone of Ile 328. Among these residues, Asp 305 (Figure 6) stabilizes the choline molecule, and Ile 328 interacts with the adenine moiety of ATP (Figure 5). The mutation of His 303 to alanine (H254A in CKA-2) prevents the formation of the hydrogen-bond pattern, and directly destabilizes Asp 305 and Ile 328. An additional destabilization of the neighboring Asp 329 that binds the Mg^{2+} ions (Figure 5) can also be expected. It must be pointed out that this hydrogen-bond pattern remains stable during the whole trajectory in simulations A and B. Finally, Asn 304 forms a hydrogen bond with Asn 336 and helps in the maintenance of the integrity of the binding sites, and in the proper orientation of the neighboring Asp 305. Again, it can be expected that mutation of this Asn 336 by alanine should maintain the initial activity while introducing time instability.

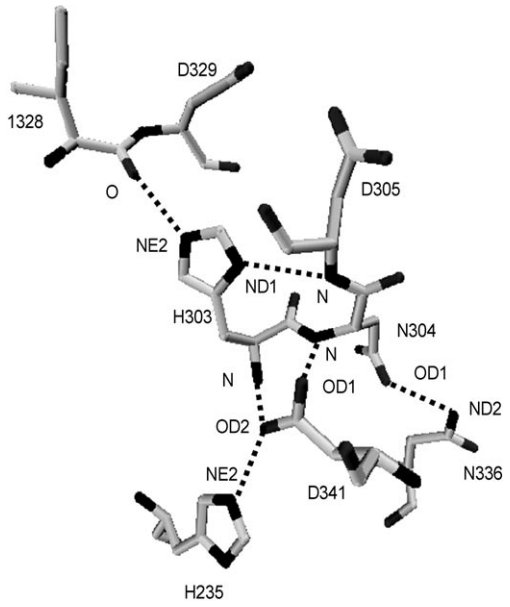

Figure 9. Hydrogen-bonds pattern involved in the stabilization of crucial residues Asp 305, Ile 328, and Asp 329 in the CK-α model. Ile 328 is involved in the interaction with the ATP adenine moiety, Asp 329 in stabilization of Mg^{2+} ions, and Asp 305 in the interaction with choline. Hydrogen atoms have been deleted for clarity.

Mutations of D255 and N245 in CKA-2 (both in the Brenner motif) dramatically affect the catalytic efficiency of this enzyme. D255A and D255Q mutants show a total loss of activity, whereas the D255E mutant still conserves a small residual activity (0.1 % k_{cat}), indicating that the carboxylate group in a precise position is essential for the catalysis. This residue is conserved in the Brenner motif of protein kinases, choline/ethanolamine kinases, and aminoglycoside phosphotransferases. This residue is also conserved in CK-α (Asp 305) and is situated near the choline molecule (Figure 7). A more profound study is necessary, including quantum mechanics, to elucidate its putative role as a base in the catalysis process. The biological importance of Asp 305 can be justified because of its proximity to the choline molecule during the whole trajectories A and B.

N260A mutation produces a CKA2 mutant enzyme with a 300-fold reduction in k_{cat}, a 36-fold increase of K_m for the Mg^{2+} ion, and a slight increase of K_m for ATP. This residue is conserved in APH(3′)-IIIa and ePKs where the corresponding asparagine interacts with a Mg^{2+} ion. In CK-α, this residue is also conserved (Asn 310) and we have found that its CO binds one of the Mg^{2+} ions during the whole trajectory in simulations A–D (Figure 5). Consequently, substitution of this residue by Ala should result in a barely decreased affinity for magnesium, a diminution of ATP affinity, and a sharp drop in k_{cat}.

Four residues have been mutated on the CKA-2 choline kinase motif. D301 is a conserved residue on many kinases, and it has been found that its biological role is to coordinate the two Mg^{2+} ions of the ATP-Mg complex through its carbonyl group. In APH(3′)-IIIa, substitution of this Asp by Asn, which potentially coordinates Mg^{2+}, lacks any detectable activity.[25] D301A, D301N, or D301E mutations in CKA-2 lead to a total loss of activity. In CK-α, this residue corresponds to Asp 329, and we have found that it can coordinate one or two of the magnesium ions (Figure 5), and hence its biological importance is confirmed by our MD simulations.

CKA-2 glutamate E303 is conserved in CK-α (Glu 331) but it does not have any apparent counterpart in other kinases. E303A mutation provokes a strong reduction of the catalytic efficiency in CKA-2, but mutations E303D or E303N are not so detrimental to activity, indicating that a CO group is necessary in this position of the enzyme. In CK-α, Glu 331 coordinates only one of the Mg^{2+} ions and, again, the precise manner of coordination depends on the presence or absence of Ca^{2+}

(Figure 5). In simulation A, Glu331 uses only one of the oxygen atoms to coordinate with magnesium, while in simulation B the two O carboxylate atoms are used. The situation described by simulations A are more compatible with mutational data since this coordination would still be possible on changing this Asp for Asn.

Another conserved residue in CKA-2 choline kinase motif is N308, which seems to be less critical for activity as mutation to Ala (N308A) produces only a threefold decrease in k_{cat}, and the substitution with Asp (N308A) or Gln (N308Q) is even less detrimental. This residue is also conserved in CK-α (Asn 336), and is involved in the stabilization of Asp 305 through the hydrogen-bond network shown in Figure 9. Asn 336 hydrogen bonds the Asn 304 side-chain carbonyl group, the neighboring residue of Asp 305. Mutation by alanine prevents such interaction and allows a higher mobility of Asn 304 and Asp 305, decreasing the activity. Nevertheless, in the mutation by Asp (or Gln), stabilization of Asn 304 can still occur through a hydrogen bond in which Asn 304 acts as a donor through its NH_2 group.

The last residue mutated in the CKA-2 choline kinase motif is E320 and it seems to play a complex role in the catalysis. Mutation E320A strongly diminishes the ATP affinity (26-fold higher K_m) without changing the value of k_{cat}, suggesting that this residue can participate in ATP binding. Further, this mutant enzyme is active for only a short time, suggesting that E320 can also play a structural role in CKA-2. Nevertheless, this amino acid is one of the residues that binds the Ca^{2+} ion in the CKA-2 crystal structure and is situated far away from the putative ATP binding site, and it is not clear how it can modify the ATP affinity. This glutamate is also conserved in CK-α (Glu 348) and in our MD simulations there is no significant difference. In simulation B, Glu 348 remains firmly coordinated with Ca^{2+} ion, and far from (more than 9 Å) ATP or Mg^{2+} ions. In simulation A, Glu 348 has a higher mobility but still remains far away from the ATP-Mg complex, and we have not yet found any explanation for the sharp drop in the K_m for ATP.

Finally, in the CKA-2 COOH-terminal only tryptophan W387 has been mutated into alanine. W387A mutant shows a low value for k_{cat} with no changes in the values of K_m. This is a conserved residue in all choline/ethanolamine kinases, but not in other kinases, suggesting that it can participate in choline binding. In our CK-α this residue is also conserved (Trp 419) and forms part of the proposed choline binding pocket that is completed by Trp 422, Tyr 332, Leu 418, and Asp 305. The three aromatic residues form a cage (Figure 7) that surrounds the choline molecule, while Leu 418 closes the back of this cage. In the other two faces of the cage are situated Asp 305 (bottom), and the outmost ATP phosphate moiety. Choline is stabilized into this cage (probably by π-cation interactions) and the high volume of these three amino acids correctly orientates the substrate for the success of the catalysis. It can be expected that the mutation of one of these residues should significantly modify the mobility of choline into the binding pocket and would probably allow a rotation of the molecule. Hence, the expected consequence of this mutation is a poor catalysis, as can be deduced from the low value of k_{cat}. As the other two aromatic residues still surround the choline molecule in the mutant enzyme, the modification of the π-cation interactions is probably not as high as to decrease the K_m for choline.

In simulation A, a wide movement of Gln 307 has been observed, in such a way that this residue forms a coordinate bond with one of the Mg^{2+} ions and also stabilizes the choline molecule by forming a hydrogen bond with the hydroxy group of this substrate (Figure 8). The question that immediately arises is if the Gln307 movement has any important role in the choline kinase inhibition by the Ca^{2+} ion. Unfortunately, CKA-2 glutamine Q257 (the equivalent of CK-α Gln 307) has not been mutated and it is not possible to confirm the role of this amino acid in the Ca^{2+} inhibition of CKA-2. At the moment we believe that this inhibition can be due to two different reasons: 1) Ca^{2+} binding introduces a higher rigidity in the enzyme, as can be seen in the evolution of the radius of gyration and backbone rmsd in simulation A, and hence makes the substrates binding more difficult; and, 2) the presence of Ca^{2+} prevents the rotation of Gln 307 and the subsequent choline stabilization by this residue.

In conclusion, the high degree of homology between CKA-2 and CK-α allows the construction of a homology model that can explain all the mutagenesis assays performed on CKA2. Consequently, putative ATP and choline binding sites proposed by Peisach et al. also seem to be confirmed by our MD study.

At present, we are using this information in the study of the CK-α inhibition by our previously reported inhibitors. Unfortunately, we have no biological data that could indicate whether the inhibition is competitive or noncompetitive. Nevertheless, the ATP binding site in CK-α is very accessible from the surface of the protein (Figure 10), and it could be supposed that inhibitors can be accommodated inside this binding site.

Even further and deeper studies are needed, preliminary docking results indicate that our inhibitors could bind into both ATP and choline binding sites, as they are long enough to fill both binding sites. As an example, Figure 9 shows the putative binding mode obtained by docking studies performed with one compound of general structure **7** ($R^4 = 1$-pyrrolidinyl). It can be observed that one pyrrolidine moiety of the molecule is inserted into the choline binding site while the other is situated in the ATP binding pocket. In this compound, the positive charge of the pyridinium N1 atom is delocalized over the pyrrolidine N atom, which becomes also positively charged. Consequently, this N atom can be stabilized inside the choline binding site by π-cation interaction with Tyr 322, Trp 419, and Trp 422, in a similar way to the stabilization of choline (Figure 9 shows that the pyrrolidine N atom almost coincides with the choline N atom). On the other hand, the first pyridinium moiety and the benzene ring of compound **7** occupy the pocket that accommodates the phosphate backbone, while the second pyridinium and pyrrolidine rings are situated over the ATP ribose unit.

Even these are preliminary results, a consequence for the design of new inhibitors can be obtained. The nature of both choline and ATP binding sites are really different, and hence new non symmetric inhibitors bearing a positively charged group that could be stabilized into the choline binding site, and a noncharged aromatic moiety that mimics the ATP ade-

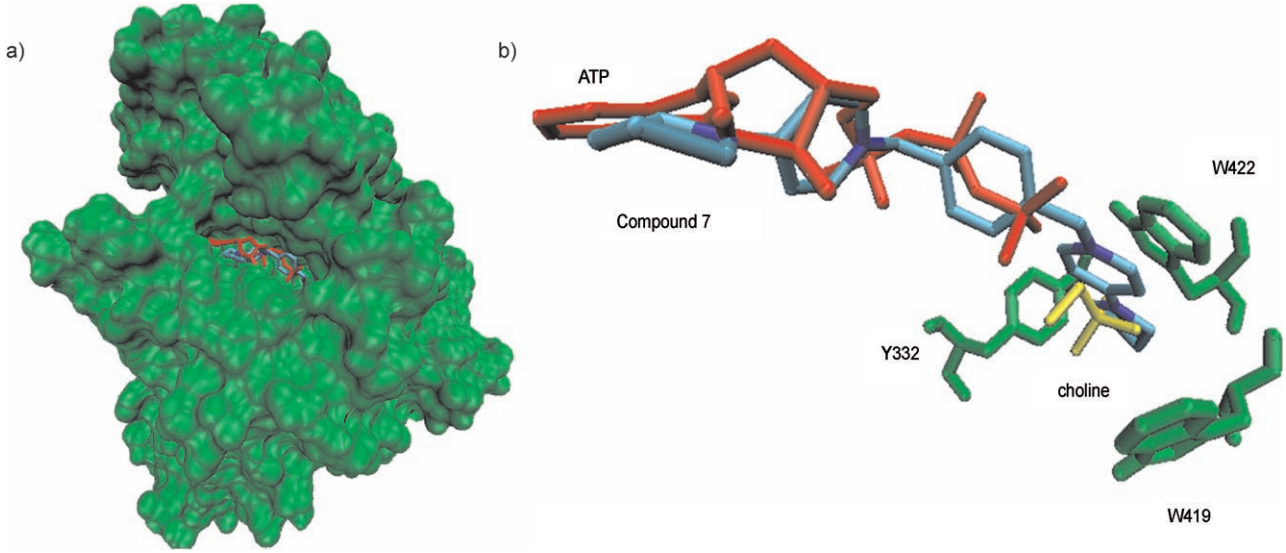

Figure 10. a) General view of compound **7** (R^4 = 1-pyrrolidinyl) docked into the CK-α model. The entrance of the ATP binding site on the protein is clearly observed. b) A detailed view of compound **7** accommodated in both ATP (red) and choline (yellow) binding sites. The positively charged N pyrrolidine atom of compound **7** almost coincides with the choline N atom.

nine moiety connected by an appropriated spacer can be designed.

Computational Methodology

CKA-2 (PDB id: 1NW1) and CK-α (Swiss-Prot code: P35790) sequences were aligned using the CLUSTALW server.[26] The secondary structure of CK-α was predicted using the Jpred[27] server at the University of Dundee.

The 3D model of CK-α was built starting from the crystal structure of CKA-2 by means of the COMPOSER module implemented in the program SYBYL.[28]

As the crystal structure CKA-2 does not have any bound substrates, Peisach et al. have proposed a putative binding site for each of both substrates (ATP and choline),[5] by comparison of the CKA-2 3D structure with the catalytic domain of APH(3′)-IIIa and PKA.

The SYBYL program was also used to prepare the initial geometries of the substrates needed for each complex, and the molecular dynamics simulations were performed using the AMBER 8.0 suite program.[29]

The ATP and the two Mg^{2+} atoms coordinates have been obtained from the crystal structure of APH(3′)-IIIa (PDB code 1J7U) complexed with phosphoaminophosphonic acid adenylate ester (ANP). Ligands were extracted from the complex, and the atom and bond types were carefully checked and adjusted to prepare the initial geometry of an ATP molecule complexed with two Mg^{2+} ions. Choline structure was built from standard fragments from the SYBYL libraries, and after proper minimization and optimization, the resulting structure was used as the starting geometry in the construction of each complex needed for the MD simulation.

The partial atomic charges for choline and for ATP·2 Mg^{2+} complex were derived from the molecular electrostatic potential (MEP) previously calculated using Gaussian98,[30] according to the RESP methodology.[31] For the protein, partial atomic charges were read from the AMBER 8.0 libraries.

Amber 2003 force field[32] was employed to define the atom types, and potentials for the protein and ATP, while the general amber force field[33] (gaff) was used to define all needed atom types and parameters for choline. For both Ca^{2+} and Mg^{2+}, previously reported parameters were used.[34]

Once the ATP·2 Mg^{2+} complex was adequately prepared, it was manually docked into the CK-α model, in a position equivalent to that of the APH(3′)-IIIa. Choline was inserted into the putative binding pocket located between helix J and the loop of the Brenner and CK motifs, and near the putative ATP binding site. When needed, the Ca^{2+} ion was extracted from the crystal structure of CKA-2 and docked onto the equivalent position of the CK-α model.

The input files for the MD simulations were prepared with the xLEaP module of Amber, reading and combining the different files containing appropriate fragments prepared as described above. Each system was solvated with a box of TIP3P water molecules which contains at least 8.0 Å of water around the solute, and neutralized by the addition of Na^+ ions. Finally, for each complex the topology and the coordinate files were written and used in the MD simulations (AMBER's Sander module).

Prior to the MD simulation, each system was energy-minimized in two stages: firstly the solvent was relaxed while all the solute atoms were harmonically restricted to their original positions with a force constant of 100 kcal mol^{-1} Å^{-2} for 1000 steps; and secondly, the whole molecular system was minimized for another 1000 steps.

Furthermore, the system was heated from 100 to 300 K during 10 ps (NTV, PBC conditions), and then equilibrated keeping both temperature and pressure constant (NTP, PBC conditions, 300 K, 1 atm) during 100 ps. Particle Mesh Ewald method was used in the treatment of the long-range electrostatic interactions. The SHAKE[35] algorithm was used to constraint the C–H bond motions and a time step of 2 fs was used.

For simulations A and B, a distance restraint (d = 2.50–3.50 Å; force constant: 20.0 kcal mol^{-1} Å^{-2}) between the choline oxygen atom and the third ATP phosphorous atom was used during the minimization and the equilibration stages, with the object of maintaining a proper orientation of both substrates.

After equilibration, a MD production stage of 2 ns (NTP, PBC conditions, 300 K, 1 atm) was performed for each system under similar conditions to the equilibration stage, and trajectories were ana-

lyzed using both the AMBER ptraj module and the molecular visualization program VMD (Visual Molecular Dynamics).[36]
Preliminary docking studies were performed on the CK-α model using Autodock 3.0 program.[37] Ligand structure was constructed using fragments from the Sybyl libraries, and a geometry optimization was tackled using the Amber force field implemented on Sybyl with the previously described additional parameters[38] for the positive charged pyridinium atom. Partial atomic charges were calculated by means of the Gasteiger[39] method, and the minimized geometry was used to prepare the ligand for its use in Autodock following the standard procedure. Potential maps were calculated by means of the Autogrid program using a grid of 60×60×60 points centered on the geometry center of both the choline and ATP binding sites. Finally, docking calculation was performed using 100 runs of the genetic algorithm implemented in Autodock and the final geometries were clustered and analyzed.

Acknowledgments

The authors gratefully acknowledge the "Centro de Servicios de Informática" of the University of Granada (Spain) for their generosity in allowing the use of their computer time and scientific software on their SGI Origin 3400 computer.

Keywords: choline kinase · homology modeling · inhibition · molecular dynamics

[1] J. H. Exton, *Ann. N. Y. Acad. Sci.* **2000**, *905*, 61 – 68.
[2] a) E. P. Kennedy, S. B. Weiss, *J. Biol. Chem.* **1956**, *222*, 193 – 214; b) L. F. Borkenhagen, E. P. Kennedy, *J. Biol. Chem.* **1957**, *227*, 951 – 962.
[3] a) P. M. Gaynor, T. Gill, S. Toutenhoofd, E. F. Summers, P. McGraw, M. J. Homann, S. A. Henry, G. M. Carman, *Biochim. Biophys. Acta* **1991**, *1090*, 326 – 332; b) D. E. Vance, *Eur. J. Med. Res.* **1996**, 182 – 188.
[4] C. Kent, *Prog. Lipid Res.* **1990**, *29*, 87 – 105.
[5] D. Peisach, P. Gee, C. Kent, Z. Xu, *Structure* **2003**, *11*, 703 – 713.
[6] C. Aoyama, K. Nakashima, K. Ishidate, *Biochim. Biophys. Acta* **1998**, *1393*, 179 – 185.
[7] A. Cuadrado, A. Carnero, F. Dolfi, B. Jimenez, J. C. Lacal, *Oncogene* **1993**, *8*, 2959 – 2968.
[8] A. Ramírez de Molina, A. Rodríguez-González, R. Gutiérrez, L. Martínez-Piñeiro, J. J. Sánchez, F. Bonilla, R. Rosell, J. C. Lacal, *Biochem. Biophys. Res. Commun.* **2002**, *296*, 580 – 583.
[9] A. Rodríguez-González, A. Ramírez de Molina, F. Fernández, J. C. Lacal, *Oncogene* **2004**, *23*, 8247 – 8259.
[10] J. Campos, M. C. Nuñez, V. Rodríguez, M. A. Gallo, A. Espinosa, *Bioorg. Med. Chem. Lett.* **2000**, *10*, 767 – 770.
[11] A. Conejo-García, J. M. Campos, R. M. Sanchez-Martin, M. A. Gallo, A. Espinosa, *J. Med. Chem.* **2003**, *46*, 3754 – 3757.
[12] A. Conejo-García, M. Báñez-Coronel, R. M. Sánchez-Martín, A. Rodríguez-González, A. Ramos, A. Ramírez de Molina, A. Espinosa, M. A. Gallo, J. M. Campos, J. C. Lacal, *J. Med. Chem.* **2004**, *47*, 5433 – 5440.
[13] R. M. Sánchez-Martín, J. M. Campos, A. Conejo-García, O. Cruz-López, M. Báñez-Coronel, A. Rodríguez-González, M. A. Gallo, J. C. Lacal, A. Espinosa, *J. Med. Chem.* **2005**, *48*, 3354 – 3363.
[14] J. Campos, R. M. Sánchez-Martín, A. Conejo-García, A. Entrena, M. A. Gallo, A. Espinosa, *Curr. Med. Chem.* **2006**, *13*, 1231 – 1248.
[15] A. Conejo-García, J. M. Campos, A. Entrena, R. M. Sánchez-Martín, M. A. Gallo, A. Espinosa, *J. Org. Chem.* **2005**, *70*, 5748 – 5751.
[16] C. Yuan, C. Kent, *J. Biol. Chem.* **2004**, *279*, 17801 – 17809.
[17] D. L. Burk, W. C. Hon, A. K. W. Leung, A. M. Berghuis, *Biochemistry* **2001**, *40*, 8756 – 8764.
[18] Y. A. Madhusudan, E. A. Trafny, N. H. Xuong, J. A. Adams, L. F. Ten Eyck, S. S. Taylor, J. M. Sowadski, *Protein Sci.* **1994**, *3*, 176 – 187.
[19] S. Brenner, *Nature* **1987**, *329*, 21 – 21.
[20] C. Aoyama, N. Yamazaki, H. Terada, H. Ishidate, *J. Lipid Res.* **2000**, *41*, 452 – 464.
[21] Verify 3D server is available at: http://nihserver.mbi.ucla.edu/Verify_3D; a) J. U. Bowie, R. Luthy, D. Eisenberg, *Science* **1991**, *253*, 164 – 170; b) R. Luthy, J. U. Bowie, D. Eisenberg, *Nature* **1992**, *356*, 83 – 85.
[22] J. Zheng, D. R. Knighton, L. F. Ten Eyck, R. Karlsson, N. Xuong, S. S. Taylor, J. M. Sowadski, *Biochemistry* **1993**, *32*, 2154 – 2161.
[23] M. C. Hutter, V. Helms, *Protein Sci.* **1999**, *8*, 2728 – 2733.
[24] In the text and Tables, one letter code has been used for denoting CKA-2 residues while three letters code refers to the CK-α amino acids. In Figures, only residues belonging to CK-α have been represented but using one letter code for simplicity.
[25] D. D. Boehr, P. R. Thompson, G. D. Wright, *J. Biol. Chem.* **2001**, *276*, 23929 – 23936.
[26] R. Chenna, H. Sugawara, T. Koike, R. Lopez, T. J. Gibson, D. G. Higgins, J. D. Thompson, *Nucleic Acids Res.* **2003**, *31*, 3497 – 3500.
[27] Jpred server is available at: http://www.compbio.dundee.ac.uk/~www-jpred; J. A. Cuff, G. J. Barton, *Proteins Struct. Funct. Genet.* **1999**, *34*, 508 – 519.
[28] SYBYL Molecular Modeling Software is available from Tripos Inc., 1699 S. Hanley Road, St. Louis, MO 63144 – 2913, http://www.tripos.com.
[29] D. A. Case, T. A. Darden, T. E. Cheatham, C. L. Simmerling, J. Wang, R. E. Duke, K. M. Luo, K. M. Merz, D. A. Wang, D. A. Pearlman, M. Crowley, S. Brozell, V. Tsui, H. Gohlke, J. Mongan, V. Hornak, G. Cui, P. Beroza, C. Shafmeister, J. A. Caldwell, W. S. Ross, P. A. Kollman, AMBER 8. University of California, San Francisco, **2004**.
[30] Gaussian 98 (Revision A.7), M. J. Frisch, G. W. Trucks, H. B. Schlegel, G. E. Scuseria, M. A. Robb, J. R. Cheeseman, V. G. Zakrzewski, J. A. Montgomery, Jr., R. E. Stratmann, J. C. Burant, S. Dapprich, J. M. Millam, A. D. Daniels, K. N. Kudin, M. C. Strain, O. Farkas, J. Tomasi, V. Barone, M. Cossi, R. Cammi, B. Mennucci, C. Pomelli, C. Adamo, S. Clifford, J. Ochterski, G. A. Petersson, P. Y. Ayala, Q. Cui, K. Morokuma, D. K. Malick, A. D. Rabuck, K. Raghavachari, J. B. Foresman, J. Cioslowski, J. V. Ortiz, A. G. Baboul, B. B. Stefanov, G. Liu, A. Liashenko, P. Piskorz, I. Komaromi, R. Gomperts, R. L. Martin, D. J. Fox, T. Keith, M. A. Al-Laham, C. Y. Peng, A. Nanayakkara, C. Gonzalez, M. Challacombe, P. M. W. Gill, B. Johnson, W. Chen, M. W. Wong, J. L. Andres, C. Gonzalez, M. Head-Gordon, E. S. Replogle, and J. A. Pople, Gaussian, Inc., Pittsburgh PA, **1998**.
[31] C. I. Bayly, P. Cieplak, W. D. Cornell, P. A. Kollman, *J. Phys. Chem.* **1993**, *97*, 10269 – 10280.
[32] Y. Duan, C. Wu, S. Chowdhury, M. C. Lee, G. Xiong, W. Zhang, R. Yang, P. Cieplak, R. Luo, T. Lee, *J. Comput. Chem.* **2003**, *24*, 1999 – 2012.
[33] J. Wang, R. M. Wolf, J. W. Caldwell, P. A. Kollman, D. A. Case, *J. Comput. Chem.* **2004**, *25*, 1157 – 1174.
[34] K. Hori, J. N. Kushick, H. Weinstein, *Biopolymers* **1988**, *27*, 1865 – 1886.
[35] J. P. Ryckaert, G. Ciccotti, H. J. C. Berendsen, *J. Comput. Phys.* **1977**, *23*, 327 – 341.
[36] "VMD—Visual Molecular Dynamics": W. Humphrey, A. Dalke, K. Schulten, *J. Mol. Graphics* **1996**, *14*, 33 – 38.
[37] G. M. Morris, D. S. Goodsell, R. S. Halliday, R. Huey, W. E. Hart, R. K. Belew, A. J. Olson, *J. Comput. Chem.* **1998**, *19*, 1639 – 1662.
[38] A. Conejo-García, J. M. Campos, A. Entrena, R. M. Sánchez-Martín, M. A. Gallo, A. Espinosa, *J. Org. Chem.* **2003**, *68*, 8697 – 8699.
[39] a) J. Gasteiger, M. Marsili, *Tetrahedron* **1980**, *36*, 3219 – 3222; b) J. Gasteiger, M. Marsili, *Org. Magn. Reson.* **1981**, *15*, 353 – 360.

Received: June 27, 2006
Published online on September 29, 2006

